Parasitol Res (2017) 116:133–141
DOI 10.1007/s00436-016-5269-x

ORIGINAL PAPER

Morphological and ultrastructural characteristics of *Myxobolus ridibundae* n. sp. (Myxosporea: Bivalvulida) infecting the testicular tissue of the marsh frog *Rana ridibunda* (Amphibia: Ranidae) in Egypt

Fathy Abdel-Ghaffar[1] · Rewaida Abdel-Gaber[1] · Sherein Maher[2] · Nashwa El Deeb[2,3] · Reem Kamel[2] · Saleh Al Quraishy[4] · Heinz Mehlhorn[5]

Received: 8 September 2016 / Accepted: 19 September 2016 / Published online: 19 October 2016

Abstract Myxozoans are one of the most economically important groups of protozoan parasites causing many serious diseases of their hosts. In the present study, a total of 60 live adult male specimens of the marsh frog *Rana ridibunda* have been randomly captured during the period of January–December 2015 in different areas at Kafr El-Sheikh Governorate, Egypt and were examined for infection by myxosporidian parasites. A total of 48 (80.0 %) out of 60 frog specimens were found to be infected with *Myxobolus* species. Parasitic infection was restricted to the testicular tissue of the examined frogs. Macroscopic cysts (plasmodia) which heavily infested different parts of the testes were recovered. Morphological and ultrastructural characteristics of these myxosporidian species were carried out using light and transmission electron microscopy. Plasmodia measured 0.16–0.53 (0.34 ± 0.01) mm in diameter. Mature spores appeared oval in frontal view, measuring 8.9–11.5 (9.6 ± 0.1) μm in length and 7.5–9.1 (8.4 ± 0.1) μm in width containing 5–6 turns of polar filaments. Morphometric characterization revealed that the very small size of the present *Myxobolus* species was the most distinctive feature that separates them from all previously described *Myxobolus* species. Ultrastructural analysis showed that the plasmodia are surrounded by a plasma membrane with numerous pinocytotic protrusions extending toward the host cell. The generative cells and the different developmental stages are arranged at the periphery of the plasmodia, while immature and mature spores are centrally located. Sporogenesis, capsulogenesis, valvogenesis, and spore maturation of the present parasite are also described. The present species is described as *Myxobolus ridibundae* and represents a new species.

Keywords *Myxobolus* spp. · Myxosporidia · Amphibia · *Rana ridibunda* · Light and electron microscopy studies

✉ Fathy Abdel-Ghaffar
fathyghaffar@yahoo.com

[1] Zoology Department, Faculty of Science, Cairo University, Cairo, Egypt

[2] Zoology Department, Faculty of Women for Arts, Science and Education, Ain Shams University, Heliopolis, Egypt

[3] Biology Department, Faculty of Science-Yanbu, Taibah University, Medina, Saudi Arabia

[4] Zoology Department, College of Science, King Saud University, Riyadh, Saudi Arabia

[5] Parasitology Institute, Düsseldorf University, Düsseldorf, Germany

Introduction

Myxozoans are the most abundant, diversified, and economically important group of parasitic protozoa. They are characterized by multicellular spores, with polar capsules containing an extrusible polar filament (Feist and Longshaw 2006; Zhang et al. 2010; Abdel-Ghaffar et al. 2012). These myxosporeans are common parasites of ectothermic vertebrates, particularly fish (Molnár and Székely 1999; Abdel-Ghaffar et al. 2005). Despite their occurrence in amphibians and reptiles, these hosts are usually not common (Eiras 2005). In addition, Wolf and Markiw (1984) demonstrated that several myxozoan species require other invertebrate hosts (usually annelids) to complete their life cycle. Over 2180 species of Myxosporea belonging to approximately 60 genera have been described (Rocha et al. 2015). Only 15 species were found in 83 representatives of the class amphibians, most of them are found in frogs and toads. Parasites described are belonging to the

genera *Myxobolus*, *Myxidium*, *Hoferellus*, *Chloromyxum*, *Caudomyxum*, and *Sphaerospora* (Fletcher 1888; Haswell 1890; Abdel-Ghaffar et al. 2012). *Myxobolus* Bütschli 1882 is the most common myxozoan genus containing approximately 850 species worldwide. Some of these parasites have been described alone upon morphological features of spores (Cleland and Johnston 1910; Eiras et al. 2005; Eiras et al. 2014). Most of these parasites are considered to be pathogenic in many different tissues and organs of fish, such as the liver, kidneys, gills, gonads, intestine, and skin (Lom and Dyková 2006). Their occurrence in amphibian gonads is difficult to estimate since these organs are not always examined during parasite monitoring (Hadfield et al. 2014). Taxonomic criteria comprising the spore morphology, exact location of sporulation, tissue specificity, host specificity, and molecular data have replaced traditional methods that have been widely used for the taxonomy of myxosporean parasites (Zhao et al. 2008; Urawa et al. 2011). According to some authors, amphibians represent an important source of protein in some European and Arabic countries. However, only rare information is available on myxozoan infections. Therefore, the present study provides data of a myxozoan infection based on morphological, morphometric, and ultrastructural data describing a testicular myxosporidian species infecting the Marsh frog *Rana ridibunda*.

Materials and methods

Samples collection and parasitological study

A total of 60 adult male specimens of the Marsh frog *R. ridibunda* (Family: Ranidae) were randomly captured by hand during the period of January–December 2015 at different areas of Kafr El-Sheikh Governorate about 134 km North of Cairo, in the Nile Delta of lower Egypt at 31° 06′ 42″ N and 30° 56′ 45″ E for latitude and longitude. All collected samples were transported alive to the Laboratory of Parasitology Research, Faculty of Science, Cairo University, Egypt, and placed for 12 h at 23 °C in a plastic food container containing 1.3 % *v*/*v* of simplified amphibian ringer (SAR: 113.0 mM NaCl, 1.0 mM CaCl2, 2.0 mM KCl, 3.6 mM NaHCO3; 220 m OSM kg–1) to distilled water. Identification of specimens was carried out according to Al-Sadoon (1988). Each frog was narcotized using chloroform. During dissection, their body cavity and internal organs were macro- and microscopically examined for the presence of parasitic infections under a stereomicroscope. To study the morphology of mature spores and to obtain taxonomical data, at least one fresh plasmodium was squeezed on a clean slide to set free spores. Fresh spores were treated with 8 % KOH solution to induce extrusion of polar filaments. For permanent preparations, air-dried smears of spores were stained with Giemsa stain. Spores were measured by help of a calibrated ocular micrometer system. All measurements were taken in micrometer as a range followed by mean ± SD in parentheses unless otherwise stated. Photomicrographs were produced using a Zeiss Axiovert 135 light microscope equipped with a Canon digital camera. Drawings were made by help of a camera lucida. Classification, measurements, and description of spores were carried out according to the guidelines of Lom and Arthur (1989). For the transmission electron microscopical study, plasmodia were fixed in 3 % glutaraldehyde in 0.1-M sodium cacodylate buffer (pH 7.4), washed in the same buffer four to five times (10 min each), post-fixed in OsO_4 (2 %) for 2 h, washed again with the same buffer, and then dehydrated in an ascending ethanol series and in propylene oxide. Finally, samples were embedded in epoxy resin. Semi- and ultrathin sections were prepared using the Reichert OMV_2 Ultratome. Semi-thin sections were stained with toluidine blue, while ultrathin sections were contrasted with uranyl acetate in 50 % ethanol followed by lead citrate and then examined in Jeol 1010-E transmission electron microscope operated at 80 kV at the Regional Centre for Mycology and Biotechnology (RCMB), Al-Azhar University, Egypt.

Results

Gross and microscopic examinations of the collected frog samples revealed that 48 out of 60 specimens of the examined frogs had been infected with myxosporidian parasites representing an infection rate of 80.0 %. Macroscopic cysts (plasmodia) of the detected myxosporidian parasites were observed in the testicular tissues of the examined samples (Figs. 1, 2). No other organs were found to be infected. The intensity of the infection was very high. More than 14 cysts with different sizes were counted per infected frog causing considerable enlargement and destruction of the testes. Seasonal variation indicated that infection generally increased during winter to 93.33 % (28/30) and decreased to 66.66 % (20/30) in summer.

Light microscopic studies

Plasmodium The infection was observed looking like tumor-like masses measuring often up to 2 cm in diameter and inducing an enormous hypertrophy to the infected organ (Figs. 1, 2). These plasmodia are whitish, ovoid, or ellipsoidal measuring 0.16–0.53 (0.34 ± 0.01) mm in diameter.

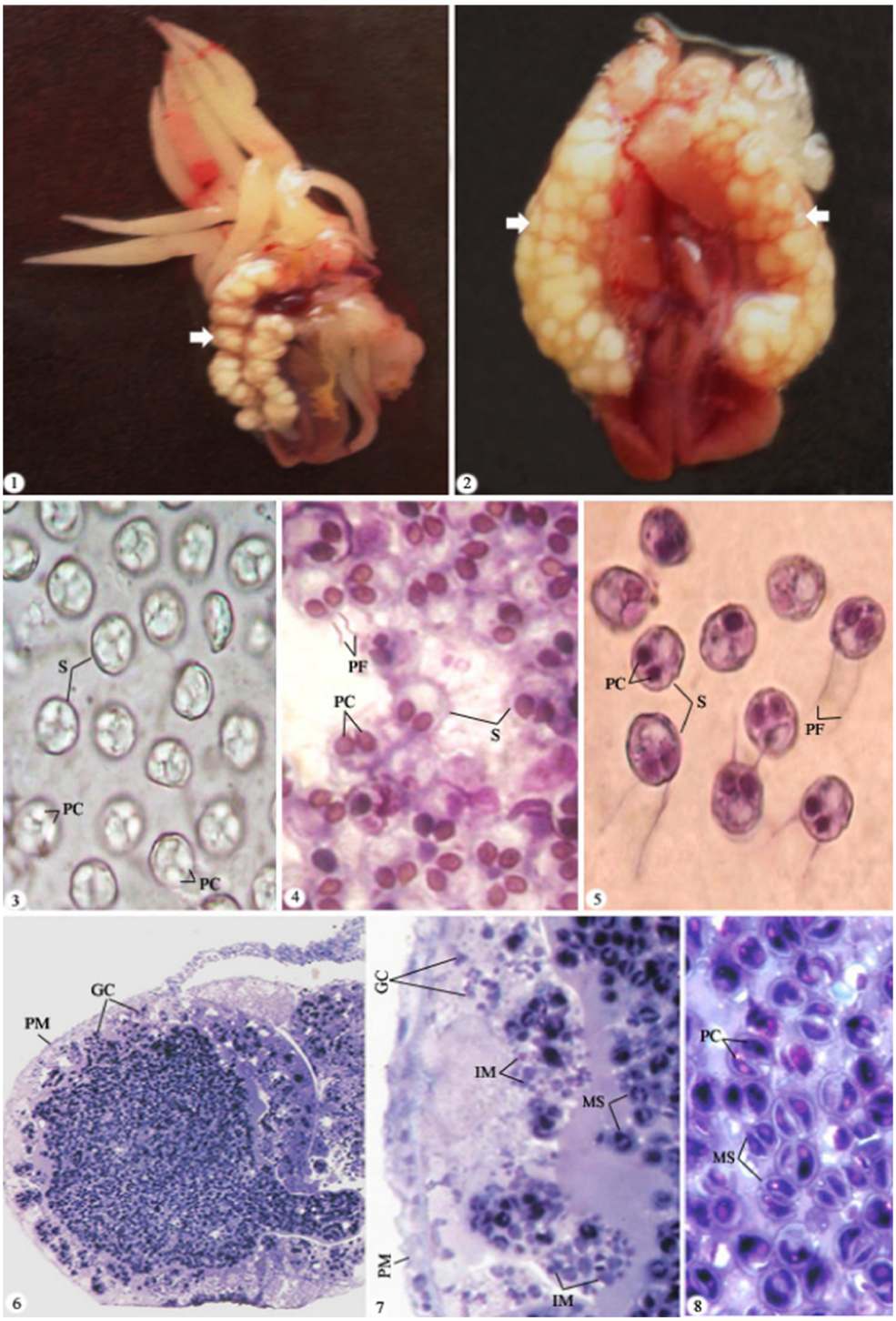

Figs. 1–8 *1,2* Photographs of heavily infected testes of the Marsh frog *R. ridibunda* with myxosporidian cysts of *M. ridibundae* n. sp. (*arrows*). *3* Photomicrographs of freshly released spores (*S*) with two polar capsules (*PC*) after squashing of plasmodia; ×1000. *4,5* Giemsa-stained spores with two darkly stained polar capsules (*PC*) and extruded polar filament (*PF*); ×1000. *6–8* Semithin sections of plasmodium stained with toluidine blue, bordered by plasmodial membrane (*PM*) followed by generative cells (*GC*) just beneath of the membrane and the core filled with different developmental stages; ×100. *7, 8* High magnifications of the peripheral part of the plasmodium encircling immature (*IM*) and mature spores (*MS*); ×400

Spore description Mature spores have an oval shape in frontal view while a biconvex shape occurs in sutural view having rounded anterior and posterior ends. They measure 8.9–11.5 (9.6 ± 0.1) μm in length and 7.5–9.1 (8.4 ± 0.1) μm in width (Figs. 3–5, 20). Both shell valves are thick, symmetrical, and 0.5 mm in thickness. Two parietal folds are present on the posterio-lateral margins of the shell valves. The two equal polar capsules are pyriform, measuring 4.3–5.9 (5.2 ± 0.1) μm in length and 2.2–3.6 (3.1 ± 0.1) μm in width. They are situated on the anterior extremity. Polar filaments form 5–6 coils arranged obliquely to the axis of the polar capsule measuring 5.3 μm in length when extruded (Figs. 4, 5). The binucleated sporoplasm is shown in Figs. 20, 21.

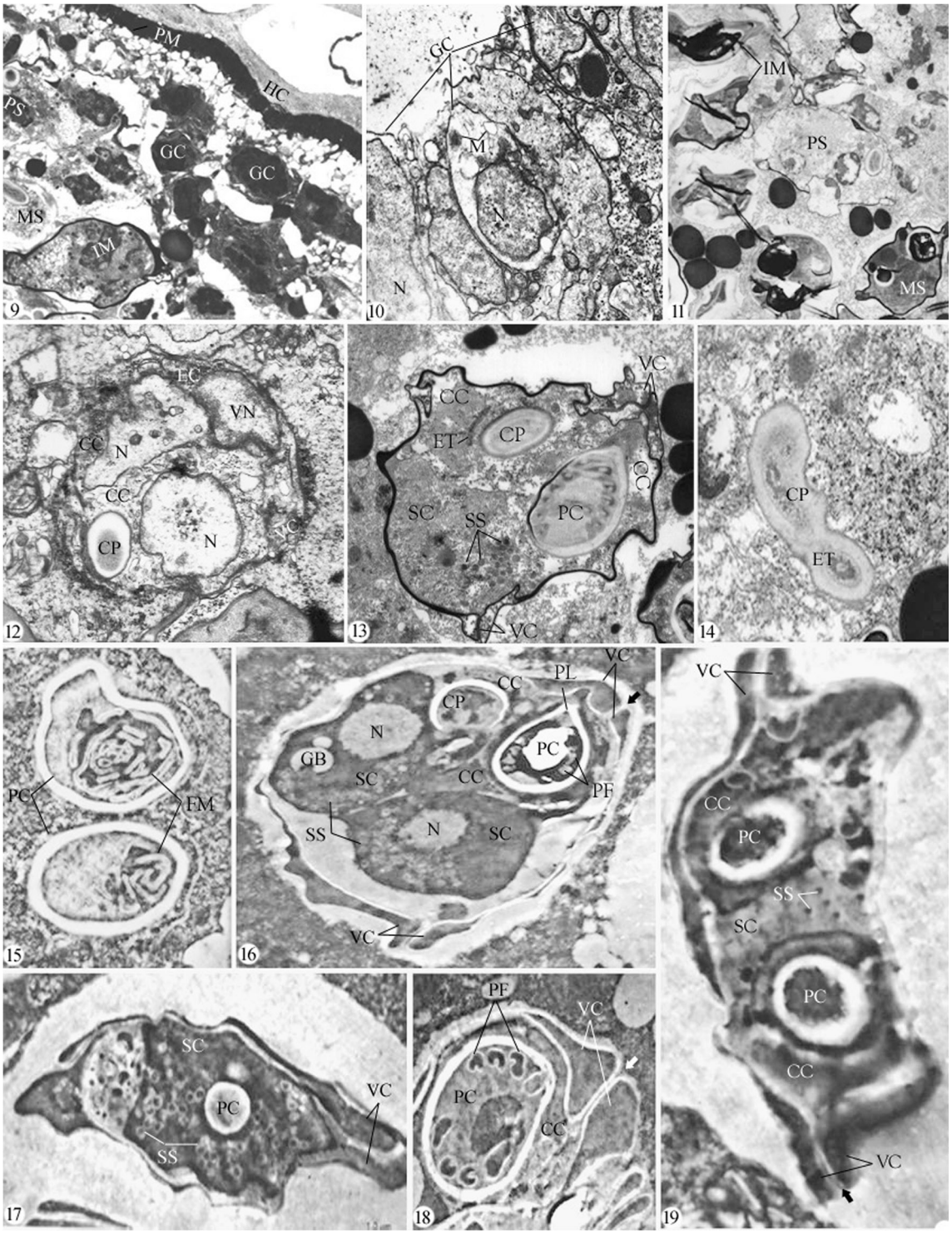

Ultrastructural characteristics

Transmission electron microscopic examination revealed that the plasmodia of the present species are bordered by a typical cell membrane (Figs. 6, 9). Numerous pinocytotic canals of various lengths protrude from this membrane into the host tissue (Figs. 9, 10). Inside of these pinocytotic canals, there occurs a broad belt of ectoplasm containing the early stages of the parasite development (Figs. 7, 10, 11). Passing inward into the plasmodia body,

Figs. 9–19 Transmission electron micrographs of plasmodia of *M. ridibundae* n. sp.: *9* Plasmodium periphery showing the plasmodial membrane (*PM*) in close contact to the host cell tissue (*HC*). Internally, several developmental stages of spores were observed such as generative cells (*GC*) situated peripherally, pansporoblasts (*PS*), immature spores (*IM*), and mature spores (*MS*); ×6000. *10* Generative cell (*GC*) with a nucleus (*N*) and few aggregations of mitochondria (*M*); ×12,000. *11* The core of the plasmodium with several developmental stages of spores such as pansporoblasts (*PS*), immature spores (*IM*), and mature spores (*MS*); ×10,000. *12* Pansporoblast containing two capsulogenic cells (*CC*) with capsular primordium (*CP*), capsulogenic nucleus (*N*), valvogenic cells (*VC*) containing valvogenic nucleus (*VN*) and surrounding by ?enveloping cell (*EC*); ×12,000. *13* Immature spore with two capsulogenic cells (*CC*) in a synchronous development as one contains mature polar capsule (*PC*), while the other in a state of primordium (*CP*). The primordium is in close contact with external tubule (ET). Note the presence of sporoplasm cell (*SC*) contains sporoplasomsomes (SS); ×12,000. *14* Earlier fusion between external tubule (*ET*) and capsular primordium (*CP*), ×20,000. *15* Section through two capsulogenic cells with two polar capsules (*PC*) in a state of complete fusion of external tubules with filament-forming materials (*FM*) appear within primordia; ×20,000. *16* Nearly mature spore showing two capsulogenic cells (*CC*) each with a polar capsule (*PC*), one of them contains coil of the polar filament (*PF*) and terminated in a capsular plug (PL) at the end of the capsule while the other still in a state of primordium (*CP*). The sporoplasm cell (*SC*) with its nucleus (*N*), sporoplasmosomes (*SS*), and glycogen bodies (*GB*); ×22,000. *17* Mature spore with polar capsules (*PC*) composed of an electron-dense outer zone, an intermediate ?translucent zone, and an inner granular cortex; ×20,000. *18* High ?magnification showing the apical zone of the spore with one polar ?capsule (*PC*) and polar filament (*PF*) arranged laterally, coiled four to six times and terminated in a capsular plug at the end of each ?capsule, and lodged in a discharge canal formed by a valvogenic cell (*VC*) with sutural ridge (*arrow*) formed between them; ×20,000. *19* Mature spores showing capsulogenic cell with two polar capsules (*PC*), sporoplasm cell with sporoplasmosomes (*SS*), and valvogenic cells (*VC*) arranged at both ends of the spore with sutural ridge (*arrow*) formed between them; ×22,000

the endoplasm contains mature and immature stages of the parasite (Fig. 8). The earliest recognizable stages of sporogenesis are the generative cells. These cells are ovoid in shape and contain a large nucleus with a prominent nucleolus and a number of mitochondrial structures (Fig. 11). The earliest pansporoblast stage seen is represented by the enclosure of a generative cell by another cell (the enveloping cell) resulting in the formation of two-celled pansporoblast stages. Subsequent development and cell divisions of the generative cells occur inside the enveloping cell resulting in the formation of two daughter sporonts within the enveloping cells (three-celled pansporoblast). Each spore-producing unit consists of capsulogenic cells and sporoplasmic cells with a sporoplasm being surrounded by valvogenic cells (Fig. 12). The early stage of capsulogenesis is characterized by polar capsules at various degrees of maturity. The first recognizable stage was characterized by the appearance of the capsular primordium as a membrane bound bulb-like electron dense structure. During early capsulogensis, external tubules characterized by an electron-dense core of granulated material can be observed inside the cytoplasm of the capsulogenic cells adjacent to the capsular primordium (Fig. 13). As follow-up of the polar capsule development, these tubules are internalized into the primordium, become shortened, and eventually disappear forming the filamentous material inside the primordium (Fig. 14). The volume of capsular primordium increases, polar filaments become coiled within the capsular cortex 5–6 times and terminate in a capsular plug (Figs. 15, 16). The development of the polar capsules is not always synchronized (Fig. 16). As soon as the capsular primordium appears, the sporoplasm can easily be recognized by the appearance of several electron-dense bodies known as sporoplasmosomes. A small area of sporoplasm in mature spores is occupied by vacuolated glycogen bodies (Fig. 17). When the spore proceeds toward maturation, the capsulogenic cell and the sporoplasm are enveloped by valvogenic cells which rapidly adhere from their ridges by help desmosomal-like junctions (Fig. 18). Then, the apex of the spore appears triangular containing numerous microtubules and large dense bodies (valve-forming bodies). In immature and mature spores, the valves appear uniformly smooth with slightly thickened ridges joined in a suture line (Fig. 19).

Taxonomic summary

Type species: *Myxobolus ridibundae* n. sp.

Type host: Marsh frog *Rana ridibunda*

Habitat and infection site: Histozoic species inhabiting testes

Type locality: Kafr El-Sheikh Governorate, Egypt

Prevalence: 48/60 (80.0 %)

Type specimens: Slides were deposited in Zoology Department, Faculty of Science, Cairo University, Egypt.

Etymology: The species name is refereeing to the host name where the parasite was discovered and described for the first time.

Discussion

It is known that amphibians represent an important source of protein for the human population in some European and Arabic countries (Fletcher 1888; Haswell 1890; Johnston 1909; Cleland and Johnston 1910; Theodorides et al. 1981a, b; Molnár and Székely 1999; Mubarak and Abed 2001). This source, however, is affected by the presence of myxosporean parasites causing many serious diseases (Lom and Dyková 2006; Abdel-Ghaffar et al. 2009; Zhang et al. 2010; Urawa et al. 2011). Salim and Desser (2000) reported that host and site of infection can be used as guidelines for recognizing the

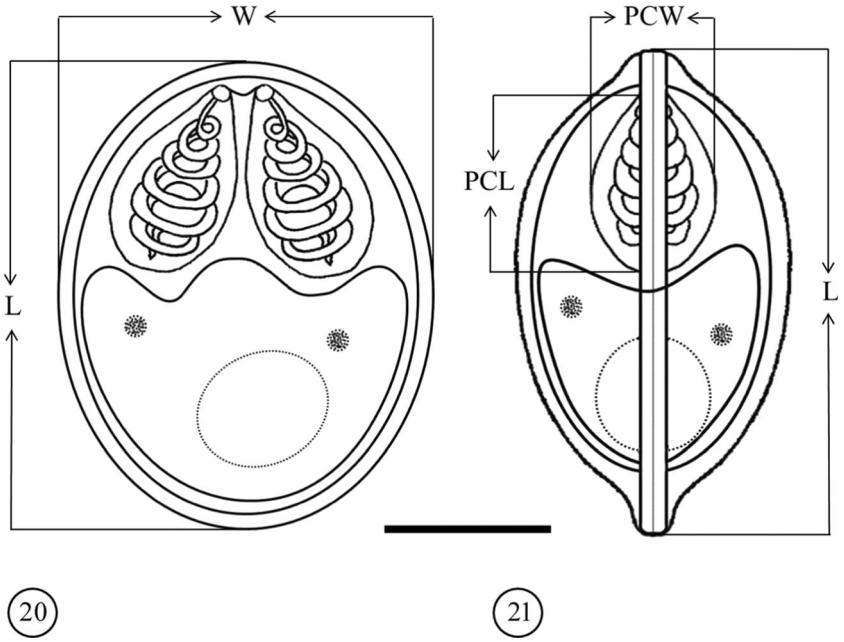

Figs. 20, 21 Diagrammatic representations of *M. ridibundae* n. sp. spores. *20* The frontal view. *21* The lateral view. *L* spore length, *W* spore width, *PCL* polar capsule length, *PCW* polar capsule width. *Scale bar* = 10 μm

previously described species when identifying new species. In the present study, the marsh frog *R. ridibunda* was found to be infected with one of the myxosporean parasites in its testicular tissue. This parasite is characterized by valve-like ellipsoidal spores with two equal valves, a biconvex shape in sutural view, a straight sutural edge, two pyriform polar capsules, and binucleated sporoplasm. All these features characterize the genus *Myxobolus* Bütschli 1882 according to the key for determination of myxosporean genera published by Lom and Dyková (2006). A review of *Myxobolus* species infecting different amphibian hosts is given in Table 1. Such hosts are *M. hylae* Johnston and Bancroft (1918) described from the testicular and urinary bladder tissues of the Golden swamp frog *Hyla aurea* in Sydney (Australia), *M. ranae* Guyenot and Naville (1922) described as tumors in the skin of Common grass frog *R. temporaria* in Switzerland, *M. chimbuensis* Ewers (1973) infecting the testes of the Anuran hylid frog *Litoria darlingtoni* from New Guinea, *M. bufonis* Upton et al. (1992) appearing as a slight constriction adjacent to seminiferous tubules of the testes of the Flat-backed toad *B. maculatus* from Cameroon, *M. fallax* Browne et al. (2002) from the testicular tissues of the Eastern dwarf tree frog *L. fallax* in Australia, *Myxobolus* sp. Szczepaniak et al. (2011) causing cutaneous myxosporidiasis in the Australian green tree frog *L. caerulea*, and *M. bufonis* Morsy et al. (2015) causing testicular myxosporidiasis infecting the Egyptian toad *B. regularis*. Morphometric characterization of the present parasite species is more or less different from the previously described parasite species. Host species and tissue localization may differentiate it from *M. hylae*, *M. ranae*, *M. chimbuensis*, *M. fallax*, and *Myxobolus* sp. in having a smaller spore size, while it is markedly larger in all dimensions than that of *M. bufonis*. In addition, it differs from the other comparable species with respect to the number of the polar filament coils since it has 5–6 turns versus 3–4 turns occurring in *M. fallax*, *M. hylae*, *M. chimbuensis*, 4–5 turns in *Myxobolus* sp., 5–7 turns in *M. ranae*, and 6–8 turns in *M. bufonis*.

Ultrastructural studies showed that the host parasite interaction is species-specific and depends on the developmental stages of the parasite (Theodorides et al. 1981a, b; Delvinquier et al. 1992; Moran et al. 1999). The ultrastructural studies of the plasmodial wall of myxosporeans are of major importance to show the characteristic features of this dangerous group of parasites (Abdel-Ghaffar et al. 2012). The plasmodia of the present examined parasite contain immature spores and sporogenic stages at the periphery, while the center is filled with mature spores, a finding which is in agreement with Abdel-Ghaffar et al. (2008). These plasmodia are bordered by a single-unit membrane which was continuous with numerous pinocytotic canals extending for a various length into the host tissue to supply various developing stages by suitable nutrients necessary for growth. These findings are in agreement with other studies (Schubert 1968; Current and Janovy 1976; Desser and Paterson 1978; Molnár and Székely 1999; Mubarak and Abed 2001; Abdel-Ghaffar et al. 2005). Sporogenesis starts in the present study with the formation of a pansporoblastic stage and other developmental stages that follow the pattern of other myxosporeans. Subsequent developmental events with cellular divisions result in a pansporoblast giving rise to sporont progeny cells followed by the differentiation of the sporont progenesis into spore-

Table 1 Measurements of *M. ridibundae* n. sp. compared with morphologically similar species (all measurements are provided in micrometer)

Comparable *Myxobolus* species	Host	Location	Site of infection	Spore		Polar capsule	
				Length	Width	Length	Width
Myxobolus hylae Johnston and Bancroft (1918)	*Hyla aurea*	Australia	Testes, oviduct and kidneys	8.8.15.5 (13.9)	8.0.10.7 (9.1)	3.3.5.2 (4.2)	2.2.3.1 (2.6)
M. ranae Guyenot and Naville (1922)	*Rana temporaria*	Switzerland	Skin	11–12	8–10	4–5	2.5–3.5
M. chimbuensis Ewers (1973)	*Litoria darlingtoni*	New Guinea	Testes	10–13 (11.9)	8–9 (8.4)	4–6 (4.7)	2–3 (2.2)
M. bufonis Upton *et al.* (1992)	*Bufo maculatus*	Egypt	Testes	8.8–9.6 (9.2)	8.6–9.4 (8.9)	3.4–4.6 (4.1)	2.0–3.4 (3.2)
M. fallax Browne *et al.* (2002)	*Litoria fallax*	Australia	Testes	12.6–14.6 (13.4)	12.6–14.6 (13.4)	3.3–4.7 (4.2)	2.1–2.8 (2.4)
Myxobolus sp. Szczepaniak *et al.* (2011)	*Litoria caerulea*	Australia	Testes	11.4	6.0	6.04	2.05
M. bufonis Morsy *et al.* (2015)	*Bufo regularis*	Egypt	Testes	6.2–8.4 (7.1 ± 0.2)	5.8–7.0 (6.3 ± 0.2)	3.0–4.2 (3.4 ± 0.2)	1.6–2.4 (1.9 ± 0.2)
M. ridibundae n. sp. (present study)	*Rana ridibunda*	Egypt	Testes	8.9–11.5 (9.6 ± 0.1)	7.5–9.1 (8.4 ± 0.1)	4.3–5.9 (5.2 ± 0.1)	2.2–3.6 (3.1 ± 0.1)

producing units. These results are in agreement with data obtained by Székely et al. (2015) and Zatti et al. (2015). The polar capsule has an ovoid to ellipsoidal shape and contains an inverted polar filament. At this stage, these capsules appear as bulb-like, dense structures known as capsular primordium being usually attached at their ends with a long external tubule. In the present study, the filament appears first in the external tubule while the capsular primordium was still filled with granules without any traces of filament. Similar results were obtained by Abdel-Ghaffar et al. (2009). The rudimentary polar filament is formed within the capsular primordium, and the external tubule is possibly formed from the dense granular material present in both structures as mentioned by Desser et al. (1983). The external tubule invaginates into the polar capsule and undergoes reorganization to become the polar filament. Similar results have been reported by Matos et al. (2005). The development of the two polar capsules is not always synchronized. In the present investigation, the plane of the junctions of valvogenic cells is manifested as a sutural line and is set in a plane perpendicular or oblique to the spore circumference. Similar findings were recorded in other myxosporean studies (Johnston 1909; Cleland and Johnston 1910; Abdel-Ghaffar et al. 2008; Zatti et al. 2015). As valvogenesis proceeds, several microtubules appear within the cytoplasm of the valvogenic cells, especially in the valve-suture forming regions (Reimschuessell et al. 2003; Zhao et al. 2008; Diamant et al. 2005). When sporoplasm maturation proceeds, an increase in the number of mitochondria occurs as well as an accumulation of glycogen particles. El-Mansy and Bashtar (2002), Matos et al. (2005) suggested that maturation of sporoplasm involves storage of metabolic reserves and acquisition of aerobic metabolism which under the proper stimulus may provide energy necessary for exsporulation and establishment of the sporont within a new host. Therefore, it can be concluded that the present parasite species represents a new species having a new host showing new locality records and thus can be named as *M. ridibundae*.

Acknowledgments The authors are thankful to the Faculty of Science, Cairo University, Cairo, Egypt, for providing all the facilities to complete this work. In addition, the authors extend their appreciations to the Deanship of Scientific Research at King Saud University for funding the work through the International Research Group Project IRG14-23.

Compliance with ethical standards Animal use followed a protocol approved and authorized by Institutional Animal Care and Use Committee (IACUC) at Zoology Department, Faculty of Science, Cairo University, Egypt.

References

Abdel-Ghaffar F, Abdel-Baki AS, El-Garhy M (2005) Ultrastructural characteristics of the sporogenesis of genus *Myxobolus* infecting some Nile fishes in Egypt. Parasitol Res 88:617–626

Abdel-Ghaffar F, Bayoumy EM, Bashtar A-R, Al Quraishy S, Morsy KS, Alghamdy A, Mehlhorn H (2008) Light and electron microscopic study on *Henneguya suprabranchae* Landsberg, 1987 (Myxozoa: Myxosporea) from *Oreochromis niloticus*, a new host record. Parasitol Res 103:609–617

Abdel-Ghaffar F, Bashtar AR, Mehlhorn H, Al-Rasheid K, Al-Olayan E, Abdel-Baki A, Morsy K (2009) Ultrastructure and host parasite relationships of *Kudoa pagrusi* (Myxozoa) infecting the heart muscles of sea bream *Pagrus pagrus* (L.) from the Red Sea. Parasitol Res 106:121–129

Abdel-Ghaffar F, Morsy K, Mehlhorn H, Bashtar AR, Shazly MA, Saad AH, Abdel-Gaber R (2012) First report of *Kudoa* species (Myxozoa: Kudoidae) infecting the spotted coral grouper *Plectropomus maculates* from the Red Sea. A light and ultrastructural study. Parasitol Res 4:1579–1585

Al-Sadoon MK (1988) Survey of the reptilian fauna of the Kingdom of Saudi Arabia II. The lizard and amphibian fauna of Riyadh province. Bull Maryland Herpetol Soc 34:85–98

Browne RK, Scheltinga DM, Pomering M, Mahony M (2002) Testicular myxosporidiasis in anurans, with a description of *Myxobolus fallax* n. sp. Syst Parasitol 52:97–110

Bütschli O (1882) Myxosporidia. In: Bronn's Klass O (ed) Tierreiches, protozoa, vol 1., pp 590–603

Cleland JB, Johnston TH (1910) The haematozoa of Australian batrachians. J Proc R Soc N S W 44:252–261

Current WL, Janovy J Jr (1976) Ultrastructure of interlamellar *Henneguya exilis* in the channel catfish. J Parasitol 62:975–981

Delvinquier BLJ, Markus MB, Passmore NI (1992) *Myxidium lesminteri* n. sp. (Myxosporea: Myxidiidae) from the gallbladder of three southern African Anura. Syst Parasitol 23:25–30

Desser SS, Paterson WB (1978) Ultrastrucutral and cytochemical observation on sporogenesis of *Myxobolus* sp. (Myxosporidia) from common shiner *Notropis coronutus*. J Protozool 25:314–326

Desser SS, Molnar K, Horvath l (1983) An ultrastructural study of the myxosporeans, *Sphaerospora angulata* and *Sphaerospora carassii* in the common carp (*Cyprinus caripo* L). J Protozool 30:415–422

Diamant A, Ucko M, Colorni A, Lipshitz A (2005) *Kudoa iwati* (Myxosporea: Multivalvulida) in wild cultured fish in the Red Sea: redescription and molecular phylogeny. Parasitology 91(5):1175–1189

Eiras JC (2005) An overview on the myxosporean parasites in amphibians and reptiles. Acta Parasitol 50:267e275

Eiras JC, Molnar K, Lu YS (2005) Synopsis of the species of *Myxobolus* Butschli, 1882 (Myxozoa: Myxosporea: Myxobolidae). Syst Parasitol 61:1–46

Eiras JC, Saraiva A, Cruz C (2014) Synopsis of the species of *Kudoa* Meglitsch, 1947 (Myxozoa: Myxosporea: Multivalvulida). Syst Parasitol 87:153–180

El-Mansy AIE, Bashtar AR (2002) Histopathological and ultrastructural studies of *Henneguya suprabranchiae* Landsberg, 1987 (Myxosporea: Myxobolidae) parasitizing the suprabranchial organ of the freshwater catfish *Clarias gariepinus* Burchell, 1822 in Egypt. Parasitol Res 88:617–626

Ewers WW (1973) *Myxobolus chimbuensis* n. sp. (Family: Myxobolidae; Cnidosporidia; Protozoa) from the testes of the hylid frog *Litoria darlingtoni*, from New Guinea. Science in New Guinea 1:16.19

Feist SW, Longshaw M (2006) Phylum Myxozoa. In: Woo, P. T. K. (ed.), Fish diseases and disorders: Protozoan and Metazoan infections. CABI Publishing, Wallingford. 1:230–296.

Fletcher AW (1888) On amyxosponidian infesting Australian frogs. Aust Ass Adv Sci 1:337

Guyenot E, Naville A (1922) Sur une myxosporidie (*Myxobolus ranae* n. sp.) et une microsporidie parasites de *Rana temporaria*. Rev Suisse Zool 29:413

Hadfield CA, Poynton SL, Clayton LA, Romero JL, Montali RJ (2014) *Kudoa* sp. (Myxozoa: Multivalvulida) in skeletal muscle of captive bullnose eagle rays, *Myliobatis freminvillei* (Rajiformes: Myliobatidae). J Zoo Wildl Med 45(4):896–905

Haswell WA (1890) A remarkable flat worm in the golden frog. Proc Linn Soc N S W 5:661–666

Johnston TH (1909) Exhibit: *Myxobolus* sp., a sporozoan parasite infesting and destroying the genital organs of the frog *Hyla aurea*. J Proc R Soc N S W 43:28–29

Johnston TH, Bancroft MJ (1918) A parasite, *Myxobolus hylae* sp. nov., of the reproductive organs of the golden swamp frog, *Hyla aurea*. Aust Zool 1:171–175

Lom J, Arthur JR (1989) A guideline for the preparation of species descriptions in Myxosporea. J Fish Dis 12:151–156

Lom J, Dyková I (2006) Myxozoan genera: definition and notes on taxonomy, life cycles terminology and pathogenic species. Folia Parasitol 53:1–36

Matos E, Tajdari J, Azevedo C (2005) Ultrastructural studies of *Henneguya rhamdi* n. sp. (Myxozoa) a parasite from the Amazon teleost fish, *Rhamdia quelen* (Pimelodidae). J Eukaryot Microbiol 52:532–537

Molnár K, Székely C (1999) *Myxobolus* infection of the gills of common bream (*Abramis brama* L.) in Lake Balaton and in the Kis-Balaton reservoir, Hungary. Acta Vet Hung 47:419–432

Moran JDW, Whitaker DJ, Kent ML (1999) A review of the myxosporean genus *Kudoa* Meglitsch, 1947, and its impact on the international aquaculture industry and commercial fisheries. Aquaculture 172:163–195

Morsy K, Semmler M, Al-Olayan E, Mehlhorn H (2015) (2015) Testicular myxosporidiasis and ultrastructural characteristics of *Myxobolus bufonis* (Myxobolidae) infecting the Egyptian toad *Bufo regularis* (Bufonidae). A light and electron microscopic study. Parasitol Res 114:3989–3997

Mubarak M, Abed GH (2001) Morphopathological changes of the testicular tissue of Egyptian toad, *Bufo regularis* (Amphibia, Bufonidae) infected with *Myxobolus* sp. (Myxozoa, Myxobolidae). Acta Parasitol 46:113–118

Reimschuessell R, Gieseker CM, Driscoll C, Baya A, Kane AS, Blazer VS, Evans JJ, Kent ML, Moran JDW, Poynton SL (2003) Myxosporean plasmodial infection associated with ulcerative lesions in young-of-the-year Atlantic menhaden in a tributary of the Chesapeake bay and possible links to *Kudoa clupeidae*. Dis Aquat Org 53:143–166

Rocha S, Casal G, Rangel L, Castro R, Severino R, Azevedo C, Santos MJ (2015) Ultrastructure and phylogeny of *Ceratomyxa auratae* n. sp. (Myxosporea: Ceratomyxidae), a parasite infecting the gilthead seabream *Sparus aurata* (Teleostei: Sparidae). Parasitol Int 64(5): 305–313

Salim KY, Desser SS (2000) Description and phylogenentic systematics of *Myxobolus* spp. from cyprinids in Algonquin park. Ontario J Eukaryot Microbiol 47:309–318

Schubert G (1968) Elektronenmikroskopische Untersuchungen zur Sporenentwicklung von *Henneguya pinnae* Schubert (Sporozoa, Myxosporidea, Myxobolidae). Z Parasitenkd 30:57–77

Szczepaniak K, Tomczuk K, Studzińska M (2011) Cutaneus myxosporidiasis in the Australian green tree frog *(Litoria caerulea*). Parasitol Res 108:489–492

Székely C, Molnár K, Cech G (2015) Description of *Myxobolus balatonicus* n. sp. (Myxozoa: Myxobolidae) from the common carp *Cyprinus carpio* L. in Lake Balaton. Syst Parasitol 91(1):71–79

Theodorides J, Pujol F, Neyrand-Deleffember F, Delsol M (1981a) New cases of testicular parasitism of amphibians by myxosporidians of the genus myxobolus. Proceedings of the zoological society of France on the effect of external factors on reproductive cycles: reproductive strategies. 7 to 9 July 1981, Caen, France. Bull Soc zool France 106:386

Theodorides J, Pujol P, Neyrand-Deleffember F, Delsol M (1981b) Nouveaux cas de parasitisme testiculaire d'amphibiens (*Bufo*,

Ptychadena) par des Myxosporidies du genre *Myxobolus*. Ann Sci Nat Zool Paris 3:63–68

Upton SJ, Freed PS, Freed DA, McAllister CT, Goldberg SR (1992) Testicular myxosporidiasis in the flat-backed toad, *Bufo maculatus* (Amphibia: Bufonidae), from Cameroon, Africa. J Wildl Dis 28: 326–329

Urawa S, Freeman MA, Johnson SC, Jones SR, Yokoyama H (2011) Geographical variation in spore morphology, gene sequences, and host specificity of *Myxobolus arcticus* (Myxozoa) infecting salmonid nerve tissues. Dis Aquat Org 96:229–237

Wolf K, Markiw ME (1984) Biology contravenes taxonomy in the Myxozoa: new discoveries show alternation of invertebrate and vertebrate hosts. Science 225:1449–1452

Zatti SA, Naldoni J, Silva MR, Maia AA, Adriano EA (2015) Morphology, ultrastructure and phylogeny of *Myxobolus curimatae* n. sp. (Myxozoa: Myxosporea) a parasite of *Prochilodus costatus* (Teleostei: Prochilodontidae) from the São Francisco River, Brazil. Parasitol Int 64(5):362–368

Zhang JY, Wang JG, Li AH, Gong XN (2010) Infection of *Myxobolus turpisrotundus* n. sp. in allogynogenetic gibel carp, *Carassius auratus gibelio* (Bloch), with revision of *Myxobolus rotundus* (S.L.) Nemeczek reported from *C. auratus auratus* (L.). J Fish Dis 33:625–638

Zhao Y, Sun C, Kent ML, Deng J, Whipps M (2008) Description of a new species of *Myxobolus* (Myxozoa: Myxobolidae) based on morphological and molecular data. J Parasitol 94:737–742